Calmodulin inhibitors from natural sources: An update

By: Rachel Mata, Mario Figueroa, Martín González-Andrade, José Alberto Rivera-Chávez, Abraham Madariaga-Mazón, and Paulina Del Valle

Mata, R., Figueroa, M., González-Andrade, M., Rivera-Chávez, J.A., Madariaga-Mazón, A., Del Valle, P. (2015). Calmodulin inhibitors from natural sources: An update. *Journal of Natural Products, 78* (3), pp. 576-586. DOI: 10.1021/np500954x

Abstract:

Calmodulin (CaM) plays a central role in regulating a myriad of cellular functions in physiological and pathophysiological processes, thus representing an important drug target. In previous reviews, our group has reported relevant information regarding natural anti-CaM compounds up to 2009. Natural sources continue to provide a diverse and unique reservoir of CaM inhibitors for drug and research tool discovery. This review provides an update of natural products with reported CaM inhibitory properties, which includes around 70 natural products and some synthetic analogues, belonging to different structural classes. Most of these natural inhibitors were isolated from fungi and plants and belong to the stilbenoid, polyketide, alkaloid, and peptide structural classes. These products were discovered mainly using a fluorescence-based method on rationally designed biosensors, which are highly specific, low-cost, and selective and have short reaction times. The effect of several antimitotic drugs on Ca^{2+}-*h*CaM is also described.

Keywords: Calmodulin (CaM) | antimitotic drugs | drug and research tool discovery

Article:

Introduction

Calmodulin (CaM) is the most important intracellular Ca^{2+}-binding protein in eukaryotic organisms. From the structural point of view, it is a small protein with only 148 amino acid residues arranged in two globular domains (N- and C-terminals), each one with two Ca^{2+}-binding sites. Both domains are connected by a flexible linker, which is involved in the interactions of CaM with its target proteins and antagonists.(1) CaM plays a central role in regulating a myriad of cellular functions in physiological and pathophysiological processes. Thus, CaM is involved in cell motility, cytoskeleton architecture and function, cell proliferation, apoptosis, autophagy, metabolic homeostasis, phosphorylation/dephosphorylation of proteins, ion channel function, reproductive processes, smooth muscle contraction–relaxation, and gene expression, to mention a few. CaM controls all these events through the modulation of more than 100 different proteins

including enzymes such as calmodulin-dependent phosphodiesterase (PDE1), nitric oxide synthases (NOS), several kinases, ion channels, and phosphatases, among others. Moreover, CaM has been associated with several pathological conditions including unregulated cell growth and smooth muscle malfunctions.(2) For example, recent findings have shown that most types of cancer are associated with elevated levels of Ca^{2+}-bound CaM (Ca^{2+}-CaM) and that some of its antagonists inhibit tumor cell invasion in vitro and metastasis in vivo.(2) As a consequence, this protein represents a potential drug target, and those agents that interfere with its modulatory properties can be considered CaM antagonists, which are also valuable tools for the study of physiological processes where the protein is involved.

A few structurally diverse natural products are CaM antagonists or inhibitors of the complexes this protein forms with its target enzymes. These products have been isolated from a wide variety of organisms from the Fungi, Animalia, Protista, and Plantae kingdoms. In previous reviews our group has reported the most relevant information regarding anti-CaM compounds from natural sources up to 2009.(3, 4) Herein, this information has been updated, emphasizing our own work.

Assays for Discovering CaM Inhibitors

CaM antagonists have been detected by several methods. The most widely used include functional enzymatic assays (FEA),(5, 6) gel electrophoresis,(7) affinity chromatography,(7, 8) site-directed mutagenesis,(9) X-ray crystallography,(10, 11) circular dichroism,(8) nuclear magnetic resonance spectroscopy,(12, 13) small-angle neutron scattering,(14, 15) isothermal titration calorimetry,(16, 17) localized surface plasmon resonance,(18) dual polarization interferometry,(19) intensity-fading matrix-assisted laser desorption/ionization mass spectrometry (IF-MALDI-MS),(20) and fluorescence-based methods including bioengineered biosensors.(21-26) The fluorescence-based methods are highly specific, low-cost, and selective and have short reaction times. In our studies, we have employed FEA with PDE1 as reporter enzyme, gel electrophoresis, and fluorescent biological sensors built with human CaM (*h*CaM). Our devices have been produced in *Escherichia coli* BL21-AI and engineered by rational design, replacing methionine, leucine, valine, or threonine in different positions by cysteine using site-directed mutagenesis; the resulting proteins were purified by hydrophobic exchange chromatography.(24-26) Thereafter, a thiol reactive fluorophore [i.e., monobromobimane (*mBBr*) or Alexa Fluor 350 (AF_{350})] was covalently attached to the cysteine residue as a fluorescent probe (Scheme 1). With these molecular tools it has been possible to correlate the conformational changes upon ligand binding to CaM with the changes in the emission properties of the labeled protein. Biosensor *h*CaM M124C-*mBBr* was built initially because the microenvironment surrounding methionine 124 is very susceptible to classical CaM inhibitors such as chlorpromazine (CPZ) and trifluorperazine (TFP).(24) Afterward, other devices were built including *h*CaM L39C-*mBBr*/V91C-*mBBr*,(25)*h*CaM M124C-AF_{350},(26)*h*CaM V91C-*mBBr*,(27) and *h*CaM T110C-*mBBr*.(28) The *h*CaM L39C-*mBBr*/V91C-*mBBr* is suitable for detecting classical and nonclassical inhibitors of CaM because the labeled recognition fluorophores are strategically located, and upon any ligand binding, quenching of the fluorescence will always be detected. Biosensor *h*CaM T110C-*mBBr* is appropriated for testing nonclassical inhibitors since the fluorophore probe is located at the flexible linker, far from sites where TFP interacts. Finally, *h*CaM M124C-AF_{350} was designed as an alternative to detect colorful classical CaM inhibitors without interfering with the response of the biosensor.

Measurements with all these biosensors are carried out in solution, quantitatively or qualitatively, as well as with high sensitivity and specificity.

Scheme 1

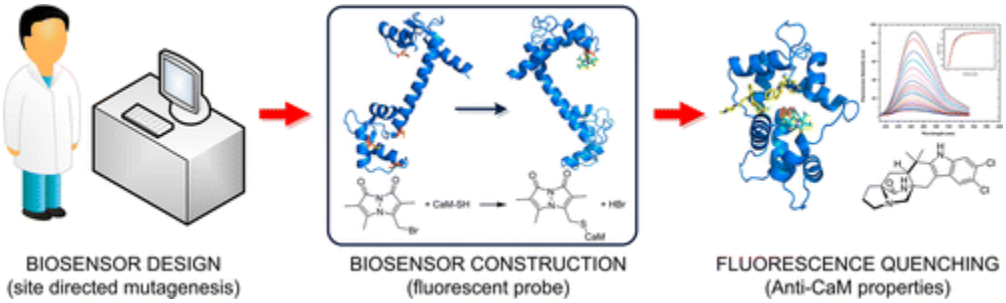

Chart 1

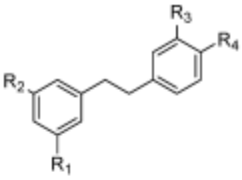

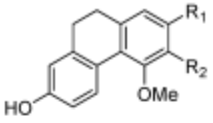

1 $R_1 = R_4 = OH$, $R_2 = R_3 = OMe$
2 $R_1 = R_3 = OH$, $R_2 = OMe$, $R_4 = H$
9 $R_1 = OH$, $R_2 = R_4 = OMe$, $R_3 = H$
10 $R_1 = R_2 = R_3 = OMe$, $R_4 = OEt$
11 $R_1 = OH$, $R_2 = OMe$, $R_3 = H$, $R_4 = N(CH_3)_2$
12 $R_1 = R_2 = OMe$, $R_3 = H$, $R_4 = N(CH_3)_2$
13 $R_1 = R_2 = R_4 = OMe$, $R_3 = H$
14 $R_1 = OH$, $R_2 = H$, $R_3 = OMe$, $R_4 = OEt$
15 $R_1 = OH$, $R_2 = R_3 = OMe$, $R_4 = OEt$
16 $R_1 = R_2 = R_3 = R_4 = H$
17 $R_1 = OH$, $R_2 = OMe$, R_3-$R_4 = OCH_2O$
18 $R_1 = OH$, $R_2 = H$, R_3-$R_4 = OCH_2O$

3 $R_1 = OH$, $R_2 = OMe$
4 $R_1 = OMe$, $R_2 = OH$

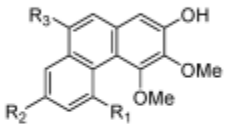

5 $R_1 = OH$, $R_2 = R_3 = H$
6 $R_1 = OH$, $R_2 = H$, $R_3 = OMe$
7 $R_1 = R_2 = R_3 = H$
8 $R_1 = H$, $R_2 = OH$, $R_3 = OMe$

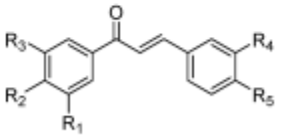

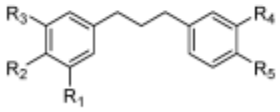

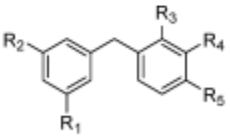

19 $R_1 = R_3 = R_4 = H$, $R_2 = OH$, $R_5 = OMe$
20 $R_1 = R_5 = OMe$, $R_2 = H$, $R_3 = R_4 = OH$
21 $R_1 = R_4 = OMe$, $R_2 = H$, $R_3 = R_5 = OH$
22 $R_1 = OH$, $R_2 = R_3 = H$, R_4-$R_5 = OCH_2O$

23 $R_1 = OH$, $R_2 = R_3 = H$, R_4-$R_5 = OCH_2O$
24 $R_1 = R_3 = R_4 = H$, $R_2 = OH$, $R_5 = OMe$
25 $R_1 = R_4 = OMe$, $R_2 = H$, $R_3 = R_5 = OH$

26 $R_1 = R_2 = R_4 = OMe$, $R_3 = OH$, $R_5 = H$
27 $R_1 = R_2 = R_4 = OMe$, $R_3 = H$, $R_5 = OH$
28 $R_1 = R_2 = R_3 = R_4 = R_5 = H$

Stilbenoids from Select Orchids

As part of our program to demonstrate the preclinical efficacy of selected Mexican medicinal plants, it was demonstrated that the extracts from the orchids *Scaphyglottis livida* (Lindl.) Schltr., *Maxillaria densa* Lindl., and *Nidema boothi* (Lindl.) Schltr. induced relaxation of the spontaneous contractions of the guinea-pig or rat ilea using ex vivo models. The IC_{50} values of these extracts ranged from 0.62 to 6 µg/mL, with maxima effects up to 90%.(29-32) Bioassay-guided fractionation of the active extracts allowed the isolation of a few bioactive bibenzyls and phenanthrenes. These metabolites also inhibited the spontaneous contractions of the isolated rat or guinea-pig ilea in a concentration-dependent form with IC_{50} values ranging from 0.33 to 7

μM.(4, 29-31) The studies conducted to determine their smooth muscle-relaxant mechanism revealed that their effects did not involve a direct interaction on the receptors of common transmitters nor any interference with Ca^{2+} influx in the cell.(29-32) However, functional assays and radioimmunoassays demonstrated that the bibenzyl compounds exerted smooth muscle-relaxant activity by the release of NO via an increase of *c*GMP levels in the rat ileum.(29) In the case of the phenanthrenes, a Ca^{2+} channel blockade partially accounted for their pharmacological effect.(33)

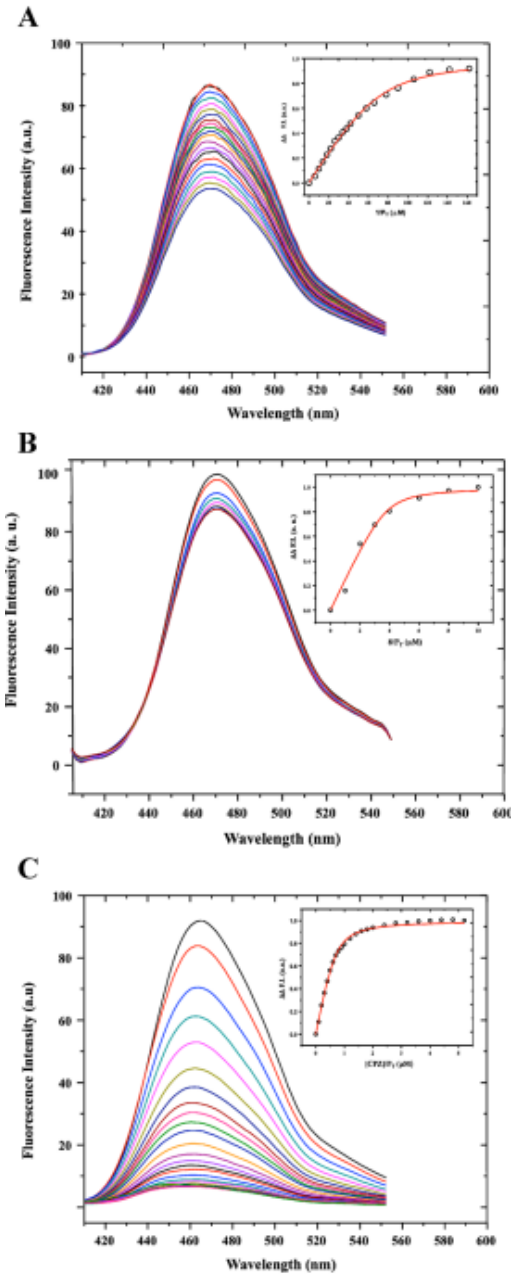

Figure 1. Fluorescence spectra and titration curves of the complexes Ca^{2+}-*h*CaM M124C-AF_{350} with (A) gigantol (**1**), (B) gymnopusin (**8**), and (C) CPZ. The absolute changes of maximal fluorescence emission were corrected for light-scattering effects and plotted relative changes in intensity (ΔΔIF) against the ligand to total protein–inhibitor complex ratio (insets).

The contraction–relaxation processes go around phosphorylation–dephosphorylation of the myosin light chain (MLC), and the equilibrium is controlled by a complex cell signaling cascade where CaM plays a central role.(34) Thus, upon any contractile stimulus, Ca^{2+} enters the cell and binds to CaM; the complex Ca^{2+}-CaM activates the myosin light chain kinase (MLCK), which in turn phosphorylates MLC, triggering smooth muscle contraction. On the other hand, smooth muscle relaxation occurs either as a result of removal of the contractile stimulus or by a direct action of a substance that stimulates inhibition of the contractile mechanisms, and regardless, the process of relaxation requires a decrease of intracellular Ca^{2+} and an increase of MLC phosphatase activity.(34) Thus, on the basis of these considerations, the effects of the stilbenoids (Chart 1) on Ca^{2+}-CaM were also investigated. In the electrophoresis assay, Ca^{2+}-CaM treated with these compounds had a lower electrophoretic mobility than the untreated protein.(31) In the functional enzymatic assays, the isolated stilbenoids inhibited the activity of the complex Ca^{2+}-CaM-PDE1 with IC_{50} values ranging from 3.2 to 36.6 μM, which was similar to the action of CPZ (IC_{50} = 10.3 μM).(31) More recently, we found that bibenzyls **1** and **2** and phenanthrenes **3**–**8** quenched the extrinsic fluorescence of the biosensors *h*CaM M124C-AF_{350} or *h*CaM M124C-*mBBr* (Table 1). The fluorescence changes were monitored between 450 and 550 nm. In all cases, the fluorescence intensity changed with increasing concentrations of the compounds. These spectroscopic changes were attributed to the formation of Ca^{2+}-*h*CaM-tested compound complexes; the phenanthrenes showed the highest affinity. For example, Figure 1 illustrates the effect provoked by gigantol (**1**), gymnopusin (**8**), and CPZ. The K_d (dissociation constant) values were 60, 0.19, and 1.0 μM, respectively. Thus, the bibenzyls and phenanthrenes of the medicinal orchids are, unequivocally, Ca^{2+}-CaM antagonists, and this effect may be related with their spasmolytic action.

Table 1. Calmodulin Inhibitors Obtained from Selected Fungi and Plants and by Synthesis As Detected by Fluorescence-Based Methods Using *h*CaM M124C-*mBBr,* *h*CaM L39C-*mBBr*/V91C-*mBBr*, *h*CaM M124C-AF_{350}, *h*CaM V91C-*mBBr*, and *h*CaM T110C-*mBBr* Biosensors and Docking Analysis

compound	K_d[a] (μM)	K_i[b] (μM)	source	ref(s)
gigantol (1)	60.8	37.0	*S. livida*, *N. boothi*	29, 31
ephemerantol B (3)	1.1	565.0	*N. boothi*, *M. densa*	30, 31
erianthridin (4)	1.4	160.0	*M. densa*	30
2,5-dihydroxy-3,4-dimethoxyphenanthrene (5)	2.2	22.1	*S. livida*, *M. densa*	29, 30
fimbriol-A (6)	1.7	65.4	*M. densa*	30
nudol (7)	1.5	42.8	*M. densa*	30
gymnopusin (8)	0.19	275.0	*M. densa*	30
3-methoxy-5-[2-(4-methoxyphenyl)ethyl]phenol (9)	80.0	109.7	synthesis	35
4-[2-(3,5-dimethoxyphenyl)ethyl]-1-ethoxy-2-methoxybenzene (10)	9.9	85.3	synthesis	35
3-{2-[4-(dimethylamino)phenyl]ethyl}-5-methoxyphenol (11)	12.0	98.1	synthesis	35
N-{4-[2-(3,5-dimethoxyphenyl)ethyl]phenyl}-*N*,*N*-dimethylamine (12)	10.0	100.1	synthesis	35
1,3-dimethoxy-5-[2-(4-methoxyphenyl)ethyl]benzene (13)	21.8	88.9	synthesis	35
3-[2-(4-ethoxy-3-methoxyphenyl)ethyl]phenol (14)	58.1	109.7	synthesis	35
3-[2-(4-ethoxy-3-methoxyphenyl)ethyl]-5-methoxyphenol (15)	25.3	124.2	synthesis	35
diphenylethane (16)	NB[c]	113.4	synthesis	35
3-[2-(1,3-benzodioxol-5-yl)ethyl]-5-methoxyphenol (17)	45.5	35.2	synthesis	35
3-[2-(1,3-benzodioxol-5-yl)ethyl]phenol (18)	63.8	13.8	synthesis	35
(2*E*)-1-(4-hydroxyphenyl)-3-(4-methoxyphenyl)prop-2-en-1-one (19)	10.3	16.2	synthesis	35
(2*E*)-3-(3-hydroxy-4-methoxyphenyl)-1-(3-hydroxy-5-methoxyphenyl)prop-2-en-1-one (20)	3.9	35.6	synthesis	35
(2*E*)-1-(3-hydroxy-5-methoxyphenyl)-3-(4-hydroxy-3-methoxyphenyl)prop-2-en-1-one (21)	5.3	23.7	synthesis	35

compound	K_d[a] (μM)	K_i[b] (μM)	source	ref(s)
(2*E*)-3-(1,3-benzodioxol-5-yl)-1-(3-hydroxyphenyl)prop-2-en-1-one (22)	ND[d]	13.5	synthesis	35
4-[3-(4-methoxyphenyl)propyl]phenol (23)	8.7	36.8	synthesis	35
4-[3-(1,3-benzodioxol-5-yl)propyl]phenol (24)	14.2	27.1	synthesis	35
4-[3-(3-hydroxy-5-methoxyphenyl)propyl]-2-methoxyphenol (25)	54.3	88.7	synthesis	35
2-(3,5-dimethoxybenzyl)-6-methoxyphenol (26)	33.8	116.8	synthesis	35
4-(3,5-dimethoxybenzyl)-2-methoxyphenol (27)	33.1	80.0	synthesis	35
diphenylmethane (28)	NB[c]	73.5	synthesis	45
malbrancheamide (29)	1.1	0.20	*M. aurantiaca*	39, 41
malbrancheamide B (30)	4.8	0.50	*M. aurantiaca*	41
isomalbrancheamide B (31)	4.8	0.50	*M. aurantiaca*	41
15-chlorotajixanthone (33)	0.03	ND[d]	*Emericella* sp. 25379	25, 43
14-methoxytajixanthone (34)	4×10^{-3}	0.03	*Emericella* sp. 25379	25, 43
shamixanthone (35)	0.24	0.08	*Emericella* sp. 25379	25, 43
tajixanthone hydrate (36)	0.09	8×10^{-3}	*Emericella* sp. 25379	25, 43
15-acetyltajixanthone hydrate (37)	0.50	3×10^{-3}	*Emericella* sp. 25379	25, 43
16-chlorotajixanthone (38)	7.3	0.08	*Emericella* sp. 25379	25, 43
tajixanthone (39)	4×10^{-3}	0.05	*Emericella* sp. 25379	25, 43
emericellin (40)	7×10^{-3}	0.14	*Emericella* sp. 25379	25, 43
variecoxanthone A acetate (41)	0.12	0.28	*Emericella* sp. 25379	25, 43
acremoxanthone C (42)	0.02	0.41	*P. lilacinum*	28
acremonidin A (43)	0.02	0.37	*P. lilacinum*	28
vermelhotin (44)	0.25	168.0	endophyte MEXU 26346	46
5-hydroxy-2,7-dimethoxy-8-methylnaphthoquinone (45)	1.6	ND[d]	*S. minimoides*	27
emodin (46)	0.33	4.7	*A. stromatoides*	47
ω-hydroxyemodin (47)	0.76	5.3	*A. stromatoides*	47
(2*S*,3*S*)-5-hydroxy-6,8-dimethoxy- 2,3-dimethyl-4*H*-2,3-dihydronaphtho[2,3-*b*]-pyran-4-one (48)	0.22	34.9	*G. polythrix*	49, 50
(2*S*,3*S*)-5-hydroxy-6,8,10-trimethoxy-2,3-dimethyl-4*H*-2,3-dihydronaphtho[2,3-*b*]-pyran-4-one (49)	0.39	13.5	*G. polythrix*	49, 50
(2*S*)-5-hydroxy-6,8- dimethoxy-2-methyl-4*H*-2,3-dihydronaphtho[2,3-*b*]-pyran-4-one (50)	2.2	52.1	*G. polythrix*	49, 50
(2*S*)-5-hydroxy-6,8,10-trimethoxy-2-methyl-4*H*-2,3-dihydronaphtho[2,3-*b*]-pyran-4-one (51)	NB[c]	ND[d]	*G. polythrix*	49, 50
5-hydroxy-6,8-dimethoxy-2,3-dimethyl-4*H*-naphtho[2,3-*b*]-pyran-4-one (52)	1.4	50.6	*G. polythrix*	49, 50
rubrofusarin B (53)	NB[c]	ND[d]	*G. polythrix*	49, 50
chaetomine (54)	0.06	1.8	*C. globosum*	
beauverolide C (55)	0.30	1.4	*I. fumosorosea*	52
beauverolide F (56)	0.40	0.63	*I. fumosorosea*	52
beauverolide I (57)	0.19	9.7	*I. fumosorosea*	52
beauverolide J_a (58)	0.08	0.39	*I. fumosorosea*	52
beauverolide L (59)	1.7	1.1	*I. fumosorosea*	52
beauverolide M (60)	3.4	9.5	*I. fumosorosea*	52
beauverolide N (61)	1.7	5.6	*I. fumosorosea*	52
vinblastine	1.7	0.29	*Catharanthus roseus*	
vincristine	0.80	0.02	*Catharanthus roseus*	
colchicine	0.50	18.4	*Colchicum autumnale*	
paclitaxel	NB[c]	NB[c]	*Taxus brevifolia*	
griseofulvin	NB[c]	NB[c]	*P. raistrickii*	

[a] Apparent constant from the fluorescence experiments.
[b] Calculated inhibition constant from docking results.
[c] NB = not binding.
[d] ND = not determined.

On the basis of the results above-discussed, more than 20 analogues of **1** were designed and synthesized to find more active *h*CaM antagonists (Chart 1).(35) The gigantol analogues **9**–**28** differed not only in the position of the hydroxy and methoxy groups along the bibenzyl core but also in the length of the linker chain joining both phenyl moieties. The bibenzyls were obtained using the Wittig reaction; the diphenylmethanes were obtained by an acid-catalyzed

intramolecular rearrangement of a benzyl phenyl ether. Finally, the oxygenated 1,3-diphenylpropanes were obtained by one-step catalytic reduction of some chalcones in acid and 10% palladium over carbon, at 60 °C.(35)

The effect of the synthetic analogues **9**–**28** on the complex Ca^{2+}-*h*CaM-PDE1 and *h*CaM M124C-*mBBr* biosensor was also analyzed (Table 1). The synthetic compounds quenched the fluorescence of the device to different extents, then revealing different affinities to Ca^{2+}-*h*CaM; their K_d values were in the range 3–80 μM. The most active were those possessing a propyl chain between the phenyl rings, inclusive of compounds **20**, **21**, and **24**. Among the bibenzyls, compounds **11**–**13** were the most potent. In general, the position of the oxygenated functions did not have a clear impact on the affinity of the compounds to the Ca^{2+}-*h*CaM complex.

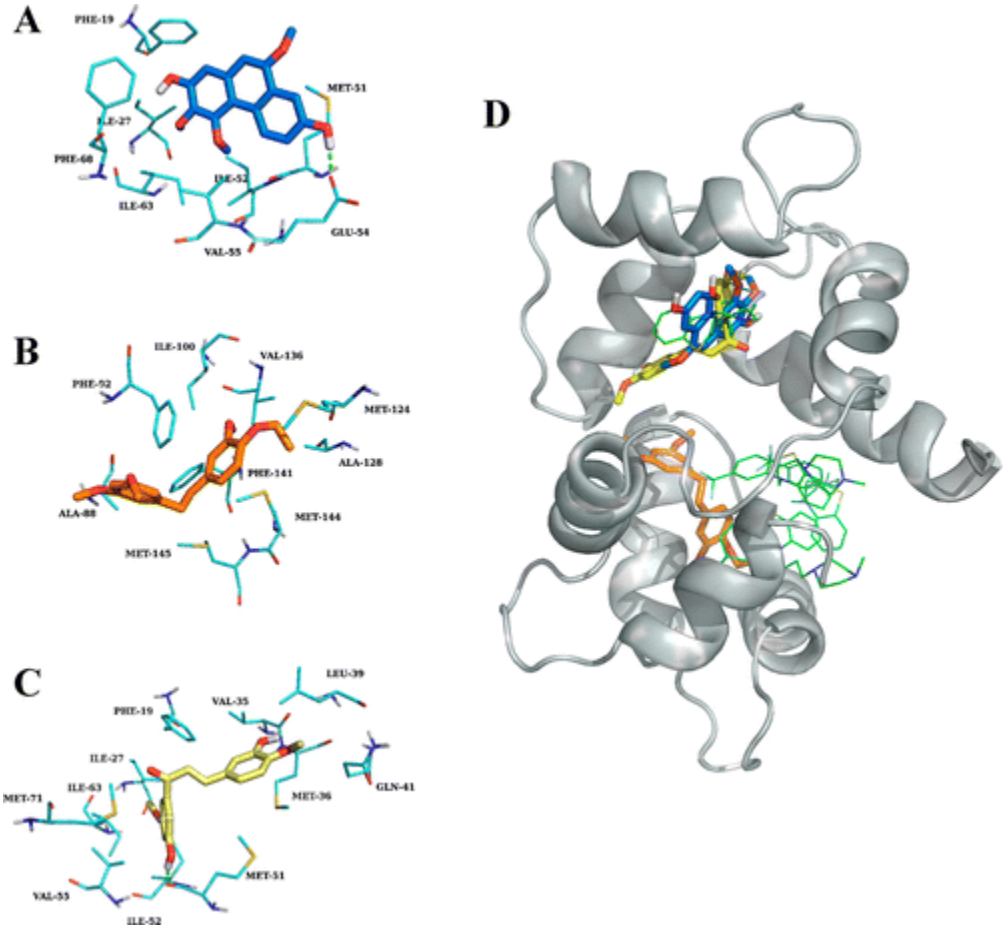

Figure 2. Predicted binding mode of (A) gymnopusin (**8**, blue sticks) and gigantol synthetic analogues, (B) **10** (orange sticks), and (C) **20** (yellow sticks), into Ca^{2+}-*h*CaM (hydrogen bonds are shown as green dashed lines). (D) Structural model of Ca^{2+}-*h*CaM-inhibitor complexes represented as gray cartoon (TFP, green lines). Amino acids involved in the interactions are shown as cyan sticks.

In order to establish the putative binding mode of the bibenzyls and phenanthrenes to Ca^{2+}-*h*CaM, docking studies were performed using the program AUTODOCK 4.0.2.(36, 37) All structures were optimized with the program Gaussian 09, using the density functional theory

method (DFT) at the B3LYP/3-21G level. Initially, the ligands were docked to the entire protein (Ca^{2+}-CaM-4TFP, PDB code 1LIN); then, the best conformations were docked in a smaller area in order to refine the results. In all cases, the two phenyl groups of the scaffold sink into the hydrophobic pockets, establishing hydrophobic and/or π–π interactions with the protein, in a similar way to TFP. As examples, docking results for compounds **8**, **10**, and **20**, the most active according to the fluorescence assay, are illustrated in Figure 2.(38)

Fungal Metabolites

In our work, fungal microorganisms have yielded the best CaM antagonists, with some of these having K_d values in the nM range. To isolate these compounds, we have pursued bioassay-guided fractionation of the active fungal extracts. Thus, once the appropriate fermentation conditions (solid or liquid media) are established, organic-soluble extracts are prepared and submitted for anti-CaM testing using *h*CaM M124C-AF_{350} or *h*CaM M124C-*mBBr*. The active extracts are fractionated until active compounds are isolated. In the next few paragraphs, selected examples are described.

Alkaloids from *Malbranchea aurantiaca*

The malbrancheamides (**29**–**32**) (Chart 2) belong to a rare family of prenylated indole alkaloids containing a bicyclic diazaoctane moiety. These compounds were isolated from the liquid culture (potato-dextrose broth, PDB) of the coprophilous fungus *Malbranchea aurantiaca* Sigler and Carmich (Myxotrichaceae). Initially, the effects of the alkaloids on CaM were assessed by gel electrophoresis and the FEA.(39-41) Most of these studies were described in our last review.(4) More recently, **29**–**32** were tested with the *h*CaM M124C-*mBBr* biosensor, and only malbrancheamide (**29**) quenched significantly (K_d = 1.1 μM) the fluorescence of the device.(41) The monochlorinated derivatives (**30** and **31**) provoked only limited decreases in fluorescence quenching, and premalbrancheamide (**32**) none. Thus, the presence of two chlorine atoms confers to **29** the best affinity to Ca^{2+}-*h*CaM.(41)

Chart 2

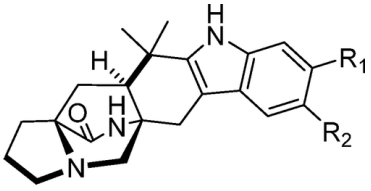

29 $R_1 = R_2 = Cl$
30 $R_1 = Cl$, $R_2 = H$
31 $R_1 = H$, $R_2 = Cl$
32 $R_1 = R_2 = H$

Docking analysis predicted that **29** is anchored in the hydrophobic pocket of Ca^{2+}-*h*CaM through hydrogen-bonding and hydrophobic interactions with a few specified amino acids of the protein.(41) To map experimentally the hydrophobic interactions in the complex Ca^{2+}-*h*CaM-**29**, HSQC experiments were performed at different mixing times. Titration of ^{15}N,^{13}C double-labeled Ca^{2+}-*h*CaM with a solution of **29** induced a diamagnetic shift of most of the methionine

methyl resonances (Figure 3). The most significant changes were observed for the methionine residues 36, 51, 71, 72, 76, 109, 124, 144, and 145, thereby corroborating the docking predictions.(41)

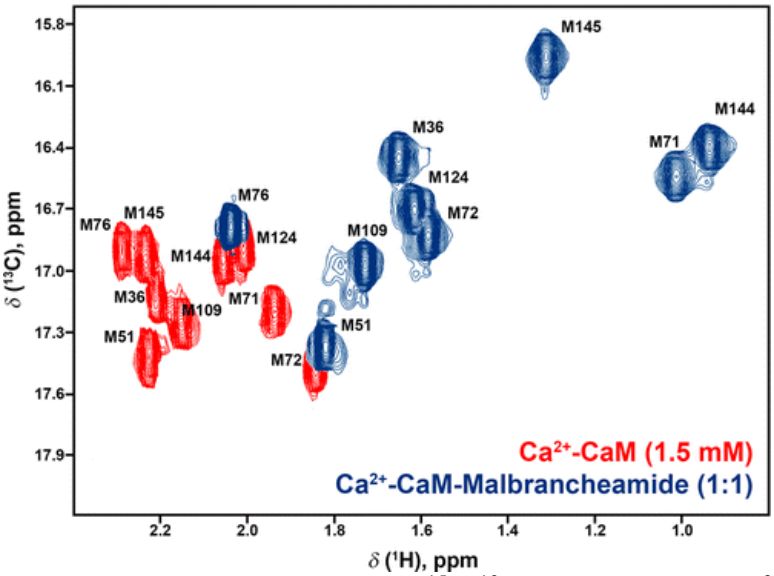

Figure 3. HSQC experiments of ^{15}N,^{13}C double-labeled Ca^{2+}-*h*CaM and after titration with malbrancheamide (**29**).

The excellent CaM inhibitory properties of **29** prompted us to investigate its smooth muscle-relaxant activity using noradrenaline (NA) precontracted rat aortal rings. The results indicated that **29** induced a vasorelaxant effect (EC_{50} = 2.7 μM) mainly by an endothelium-dependent pathway, with maximum effects of almost 100%.(42) In the absence of a functional endothelium, the effect of **29** (EC_{50} = 42.1 μM) was reduced but still significant. Experimental pharmacological evidence ruled out the COX pathway, the participation of K^+-channels, and a direct cholinergic action in the relaxation effect of **29**. However, the involvement of the NO-*c*GMP pathway was demonstrated clearly.(42) Although other mechanisms could be involved in the endothelium-independent relaxation, the fact that **29** was demonstrated as a well-characterized CaM antagonist led us to postulate that its mode of action could implicate also an interference with CaM or the contractile proteins modulated by CaM, e.g., MLCK. Therefore, the effect of **29** on two Ca^{2+}-*h*CaM target protein complexes [Ca^{2+}-*h*CaM-PDE1A and Ca^{2+}-*h*CaM-MLCK] was examined using the fluorescent biosensor *h*CaM M124C-*mBBr*.(26) CPZ was also used as a control for these experiments. The results revealed that **29** and CPZ perturbed the Ca^{2+}-*h*CaM-PDE1A and Ca^{2+}-*h*CaM-MLCK complexes since quenching of the fluorescence was observed upon titration with both inhibitors (Figure 4); compound **29** exhibited a higher affinity for the complex Ca^{2+}-*h*CaM-PDE1A (K_d = 0.28 μM) than for Ca^{2+}-*h*CaM-MLCK (K_d = 0.55 μM). On the other hand, as compared with **29**, CPZ showed slightly less affinity for the two complexes (K_d = 1.1 and 0.61 μM, respectively).(43) The disruption of the complex Ca^{2+}-*h*CaM-MLCK induced by **29** could also account for its vasorelaxant effect. Moreover, the differential affinity of **29** and CPZ for the two *h*-CaM complexes could be relevant for designing specific drugs where a particular Ca^{2+}-*h*CaM target protein complex is involved.(43)

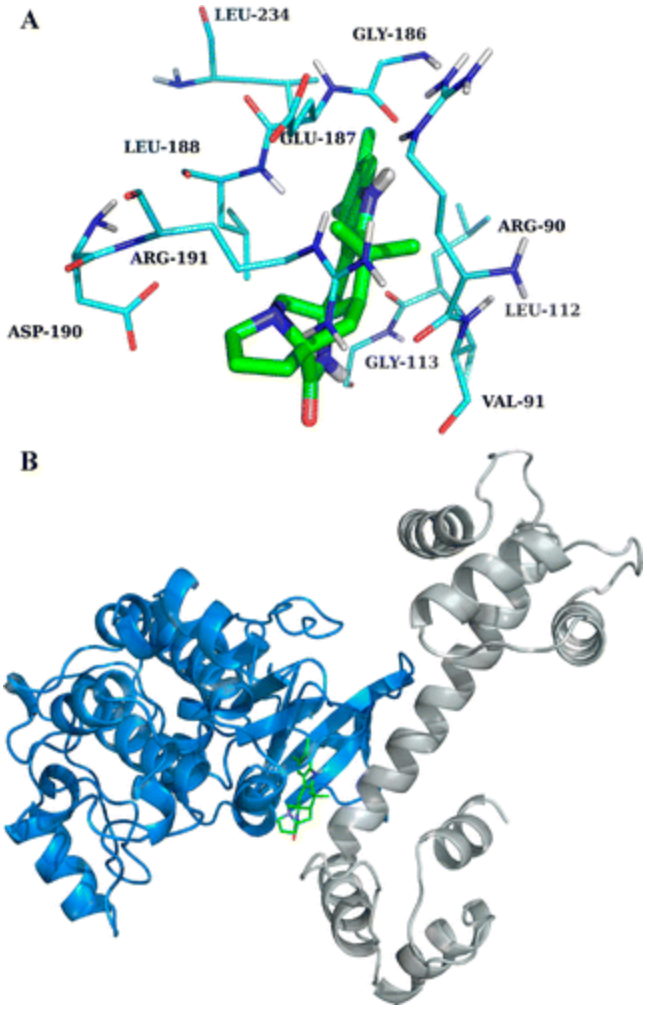

Figure 4. Predicted binding mode of (A) malbranchueamide (**29**) (green sticks) into Ca^{2+}-*h*CaM-MLCK. (B) Structural model of Ca^{2+}-*h*CaM-MLCK-**29**. Ca^{2+}-*h*CaM is represented as gray cartoon and MLCK in orange. Amino acids involved in the interactions are shown as cyan sticks.

Polyketide-Type Compounds from Selected Fungal Species

The new marine *Emericella* sp. strain MEXU 25379 (Trichocomaceae), isolated from the coral *Pacifigorgia rutilia*, collected in the Marietas Islands on the Mexican Pacific coast, biosynthesizes the prenylated xanthones **33**–**41** (Chart 3). Most of these secondary metabolites have a pyran ring fused at C-6/C-7 of the xanthone core and a prenylated chain at C-4 with different oxidation levels.(25, 44) When tested with the *h*CaM L39C-*mBBr*/V91C-*mBBr* biosensor, all compounds but **38** were found to bind to the protein with K_d values in the nM range, which is unusual for CaM inhibitors.(25) Xanthones **34**, **40**, and **33** showed the best affinity to the biosensor (K_d = 3.7, 6.8, and 28.7 nM, respectively). The results revealed also that small structural differences of these ligands greatly affect the affinity to *h*CaM. Thus, comparing the K_d values of compounds **40** and **41** (124.7 nM), as well as those of **33** and **40**, showed that the presence of an isoprenyl chain at C-4 and opening of the pyran ring increased the affinity for the protein. On the other hand, contrasting the K_d values of **34**, **35** (235.1 nM), and **36** (93.0 nM) showed that the presence of any substituent at C-14, as in compound **35**, or opening of an epoxy

functionality, as in **36**, decreased the affinity to the Ca^{2+}-*h*CaM complex. Moreover, replacement of the OH group at C-16 for a chlorine group, as in **38** (K_d = 7.3 μM), decreased the affinity toward the complex. Finally, docking studies predicted all xanthones but **38** and **40** bind to *h*CaM like TFP does, having hydrogen bonds and hydrophobic interactions that stabilized the Ca^{2+}-*h*CaM-ligand complexes.(25)

Chart 3

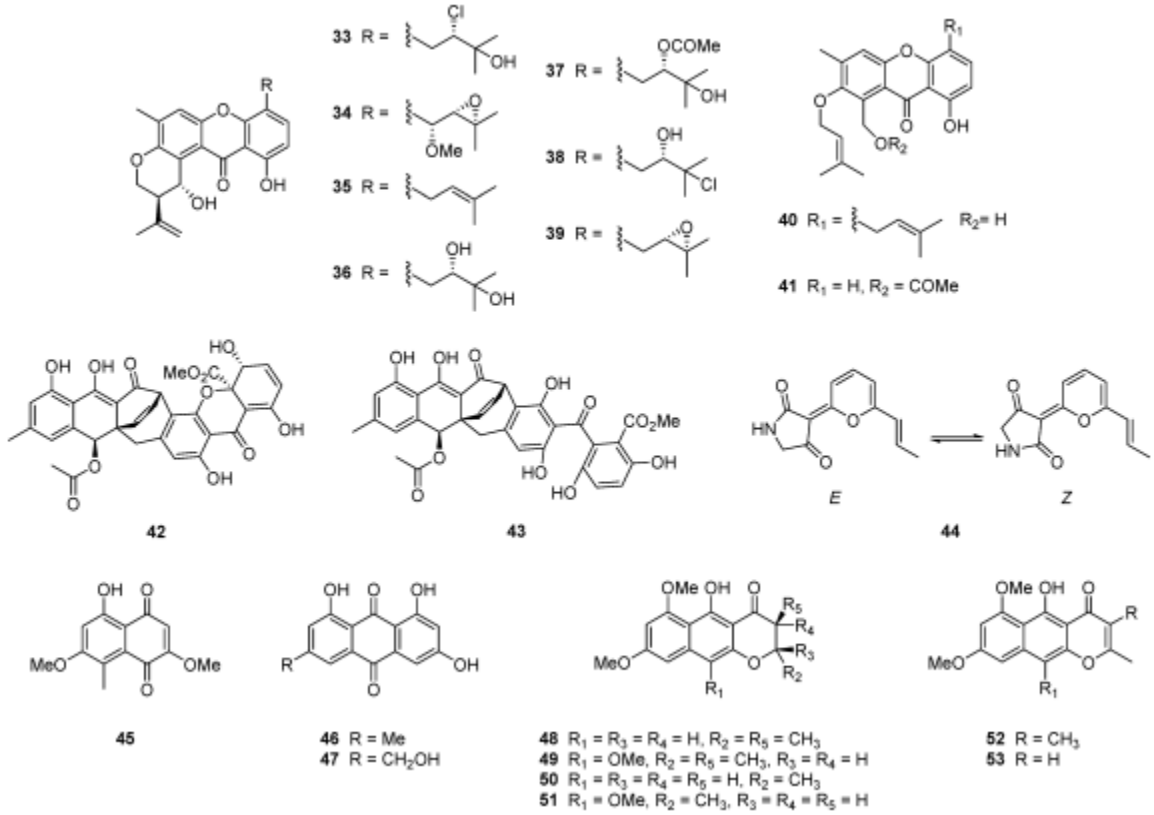

Other fungal compounds binding to Ca^{2+}-*h*CaM in the nM range were acremoxanthone C (**42**) and acremonidin A (**43**) (Chart 3), which were isolated recently from the PDB culture of *Purpureocillum lilacinum* (Thom) Luangsa-ard, Houbraken, Hywel-Jones & Samson (Ophiocordycipitaceae), a saprobic filamentous fungus isolated from the soil and some insects.(28) These two xanthone–anthraquinone heterodimers bind to *h*CaM M124C-*mBBr* with K_d values of 18.3 and 19.4 nM, respectively, 70-fold lower than that of CPZ. Docking analysis predicted that **42** binds to Ca^{2+}-*h*CaM at a similar site to the vinblastine analogue KAR-2, which is uncommon.(28, 45) The higher percentage of quenching and fluorescence maximum displacement caused by **42**, when tested with *h*CaM T110C-*mBBr*, supported the unusual binding site predicted by the docking study. As in the case of KAR-2, compound **42** might not inhibit most of the modulatory properties of *h*CaM. The cytotoxic effects displayed by **42** and **43** may be related to their anti-CaM properties.(46)

The next example refers to an interesting water-soluble polyketide characterized as vermelhotin (**44**) (Chart 3), which was isolated from a new endophytic fungal strain, MEXU 26343 (Pleosporales), associated with *Hintonia latiflora* (Sessé et Moc. ex DC.) Bull.

(Rubiaceae).(47) This compound undergoes an interconversion between the *E*/*Z* isomers, forming an equilibrium with a ratio of 1:1. The affinity of **44** (K_d = 0.25 μM) with Ca^{2+}-*h*CaM in solution was measured using the *h*CaM M124C-*mBBr* biosensor. The docking analysis predicted that both the *E* and *Z* isomers interacted with Ca^{2+}-*h*CaM at the same site as TFP, displaying mainly hydrophobic interactions with Phe92, Met109, Met124, Glu127, Ala128, and Met144 and one hydrogen bond with Glu127.(47)

According to the Lorke test,(48) compound **44** was nontoxic to mice when given orally up to 5 g/kg and exhibited a significant phytogrowth inhibitory effect when tested against *Amaranthus hypochondriacus* (IC_{50} = 141 μM vs 223 μM for Rival), *Echinochloa crusgalli* (IC_{50} = 50 μM vs 12.28 μM for Rival), *Medicago sativa* (IC_{50} = 358 μM vs 914 μM for Rival), and *Ipomea purpurea* (IC_{50}= 361 μM vs 202 μM for Rival). Whether or not this effect is related to its anti-CaM action, as has been demonstrated for ophiobolin A, remains an open question.

Another endophyte isolated from *H. latiflora* was *Sporormiella minimoides* S.I. Ahmed & Cain (Sporormiaceae) [=*Preussia minimoides* (S.I. Ahmed & Cain) Valldos. & Guarro]. This fungus, also cultured in rice, yielded several new polyketides of the corymbiferone family.(27) All compounds were tested as potential Ca^{2+}-*h*CaM inhibitors, but only the naphthoquinone **45** (Chart 3) quenched significantly the extrinsic fluorescence of the *h*CaM V91C-*mBBr* biosensor, with a K_d value of 1.6 μM. Refined docking analysis predicted that it binds to Ca^{2+}-*h*CaM at the classical site, displaying hydrophobic interactions with several amino acids.(27)

Bioassay-guided fractionation of an active extract of the marine-derived fungus *Aspergillus stromatoides* Raper & Fennell (Trichocomaceae) led to the isolation of the anti-CaM anthraquinones emodin (**46**) and ω-hydroxyemodin (**47**) (Chart 3), along with citrinin, methyl 8-hydroxy-6-methyl-9-oxo-9*H*-xanthene-1-carboxylate, and coniochaetone A.(49) Compounds **46** and **47** quenched the fluorescence of *h*CaM M124C-*mBBr* in a concentration-dependent manner with K_d values of 0.33 and 0.76 μM, respectively. Docking analysis revealed that both compounds bind to the same pocket of CPZ.(49) The *h*CaM inhibitory property of these compounds could be correlated with their widely described antineoplastic and anti-inflammatory activities, as well as their effect on several CaM-dependent enzymes such as mitogen-activated protein kinase (MAPK), protein kinase C (PKC), and MLCK.(50)

From the coprophilous fungus *Guanomyces polythrix* M.C. González, Hanlin & Ulloa (Chaetomiaceae), a number of phytotoxic naphthopyranones (**48**–**53**) (Chart 3) were obtained.(51-53) The anti-CaM properties of these compounds have been explored using different procedures. More recently, their ability to quench the extrinsic fluorescence of *h*CaM M124C-AF_{350} was assessed. The results indicated that compounds **48**–**50** and **52** bind to the protein with K_d values at the μM level, with compounds **49** and **50** having the strongest affinities (K_d = 0.39 and 2.2 μM, respectively). Molecular docking analysis of all active compounds (**48**–**50** and **52**), using a crystal structure of *h*CaM (Ca^{2+}-*h*CaM-2TFP, PDB code 1A29), showed that all bind to the same site as TFP, with hydrophobic interactions stabilizing the complexes.

Epipolythiodioxopiperazine and Peptides

Bioassay-guided fractionation of an active organic extract of *Chaetomium globosum* Kunze & Schmidt (Chaetomiaceae), a maize pathogenic fungus, led to the separation of the epipolythiodioxopiperazine chaetomine (**54**) (Chart 4). Compound **54** binds to the *h*CaM M124C-AF_{350} biosensor with a K_d value of 57 nM, 11-fold higher than TFP. Molecular docking predicted that **54** interacted with Ca^{2+}-*h*CaM in a similar manner to KAR-2 (Figure 5).

Chart 4

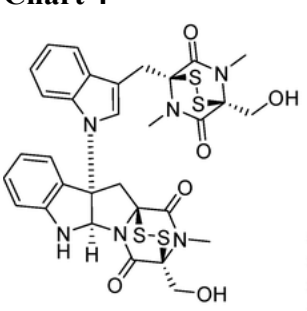

54

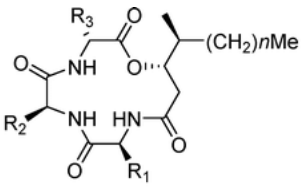

55 R_1 = R_2 = Phe, R_3 = Ile, n = 5
56 R_1 = R_2 = Phe, R_3 = Ile, n = 3
57 R_1 = Phe, R_2 = Ala, R_3 = Leu, n = 3
58 R_1 = Trp, R_2 = Phe, R_3 = Ile, n = 3
59 R_1 = Phe, R_2 = Ala, R_3 = Ile, n = 5
60 R_1 = Val, R_2 = Ala, R_3 = Leu, n = 3
61 R_1 = Tyr, R_2 = Ala, R_3 = Leu, n = 3

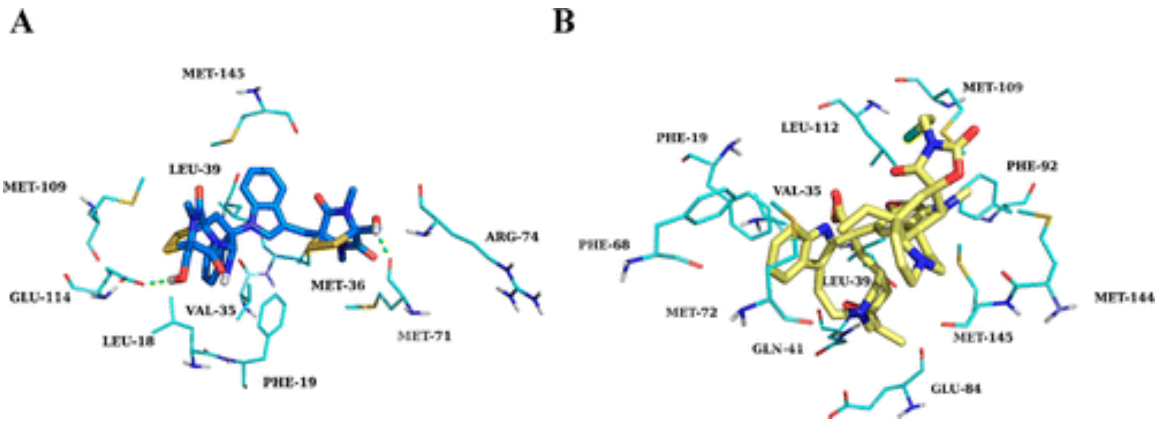

Figure 5. Predicted binding mode of (A) chaetomin**e** (**54**) (blue sticks) and (B) KAR-2 (yellow sticks) into Ca^{2+}-*h*CaM (hydrogen bonds are shown as green dashed lines). Amino acids involved in the interactions are shown as cyan sticks.

Seven lipophilic and neutral cyclotetradepsipeptides, namely, beauverolides C (**55**), F (**56**), I (**57**), J_a (**58**), L (**59**), M (**60**), and N (**61**) (Chart 4), were obtained from *Isaria fumosorosea* Wize (Ascomycota) [syn: *Paecilomyces fumosoroseus* (Wize) A.H.S. Br. & G. Sm.], an entomopathogenic fungus isolated from the whitefly.(26) These peptides showed prominent anti-CaM activity as revealed in testing with *h*CaM M124C-AF_{350}; their K_d values ranged from 0.08 to 3.4 μM. The most active compound, **58**, was almost 10-fold more active than CPZ. It is noteworthy that **58** is the only compound in the series with a tryptophan moiety in its structure.(26)

Docking of beauverolides **55**–**61** into Ca^{2+}-*h*CaM suggested that, in all cases, they bind in the same pocket as CPZ. The residues involved in the interactions comprise Glu14, Ala15, Leu18, Phe92, Ile100, Leu105, Leu109, Glu114, Met124, Ile125, Glu127, Ala128, Phe141, and Met144.

The binding forces in all cases were mainly hydrophobic in nature, since non-hydrogen bond formation was detected.(26)

During the course of the investigations described above, many other secondary metabolites from fungi were tested as Ca^{2+}-*h*CaM inhibitors, but they failed to quench the fluorescence of the different biosensors. These compounds included the indole alkaloid brevianamide A from *Penicillium brevicompactum*, which has been proposed as a biosynthetic precursor of the malbrancheamides; the polyketides mycophenolic acid, brefeldin A, citrinin, griseofulvin, and fimetarone A from *P. brevicompactum*, *Curvularia pallescens*, *A. stromatoides*, *P. raistrickii*, and *Chaetomium* sp., respectively; and, finally, aphidicolin, a tetracyclic diterpene from *Nigrospora oryzae*.

Selected Alkaloids from Plants

Berberine

The isoquinoline alkaloid berberine (**62**) (Chart 5), isolated from various plant species, possesses a number of biological activities including antibacterial, anti-inflammatory, and antineoplastic effects.(54) Several mechanisms have been proposed to explain the potential anticancer activity of **62** such as direct interaction with DNA or RNA, regulation of gene expression, and augmentation of reactive oxygen species.(54) Recently, it was demonstrated that CaM, cytochrome P450 3A4, sex hormone-binding globulin, and carbonic anhydrase II are potential targets of **62**. The investigation was initially conducted with a computational pipeline based on a ligand–protein inverse docking program (INVDOCK) and mining of the Connectivity MAP data. INVDOCK is a ligand–protein inverse docking algorithm, which could predict potential target proteins of a small molecule by attempting to dock it to known ligand-binding pockets of each of the protein entries in the PDB database. The anti-CaM property predicted for **62** was then confirmed with an FEA with PDE1 as reporter enzyme (IC_{50} = 39.7 μM). In addition, flow cytometric analysis revealed that the berberine-induced G1 cell cycle arrest in Bel7402 cells was enhanced by cotreatment with CaM inhibitors such as TFP. Western blotting data indicated that **62** decreased phosphorylation of CaM kinase II and blocked subsequent MEK1 activation as well as p27 protein degradation. These results suggested that CaM might play a crucial role in the induction of cell cycle arrest in cancer cells.(54)

Brucine and Tetrahydropalmatine

A rapid and sensitive method to detect Ca^{2+}-CaM ligands was described by Ma and co-workers(20) based on IF-MALDI mass spectrometry, which is a powerful tool to detect the formation of protein–organic compounds and protein–nucleic acids, as well as discover ligands in biological extracts for the screening of protein ligands. The method is based on a selective decrease (fading) of the ion abundance of specific ligands after the addition of the target protein, in this case Ca^{2+}-CaM. Testing of berbamine (**63**), tetrandrine (**64**), papaverine (**65**), reserpine (**66**), brucine (**67**), and tetrahydropalmatine (**68**) (Chart 5) resulted in a relative intensity fading (IF) after the addition of bovine Ca^{2+}-CaM, indicating that they bind to the protein. The relative IF was determined by comparison with the nonbinding drug propranolol. On the other hand, strychnine and piperine had either no or a weak interaction with Ca^{2+}-CaM using the same

procedure. Competitive experiments were also performed with the IF-MALDI mass spectrometry method. It is important to point out that this is the first report of the anti-CaM properties of alkaloids **67** and **68**.(20)

Chart 5

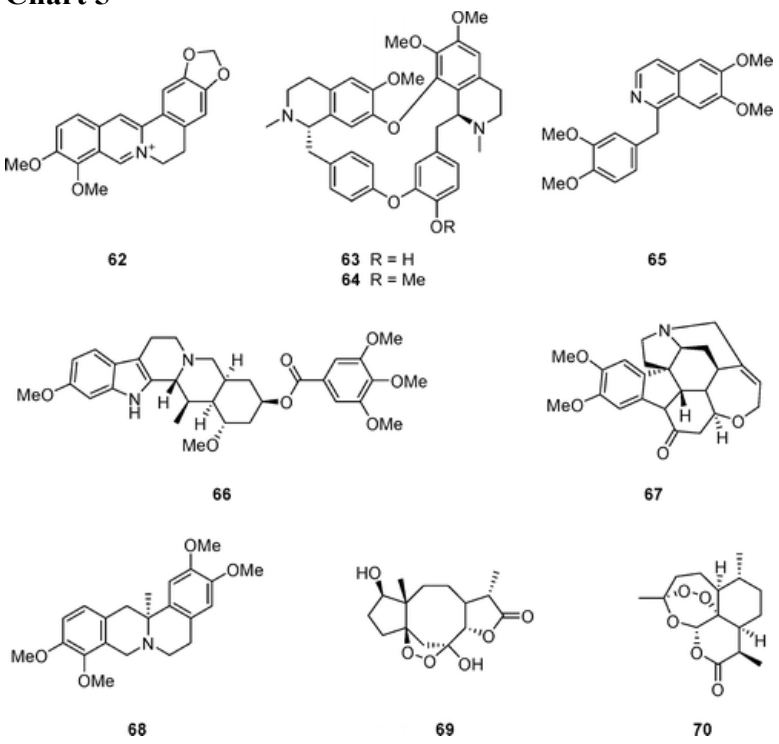

Selected Flavonoids

A few structurally related flavonoids (flavone, 3-hydroxyflavone, 6-hydroxyflavone, 7-hydroxyflavone, chrysin, quercetin, naringenin, and 6-hydroxykaempferol 3,7-dimethyl ether) showed CaM inhibitory activities in the Ca^{2+}-CaM-PDE1 assay (IC_{50} values from 5.2 to 102.3 μM).(55) These flavonoids displayed also an important vasorelaxant effect, indicating that their mode of action could involve an anti-CaM activity or an interference with contractile proteins modulated by CaM, as in the case of malbrancheamide (**29**).

Sesquiterpene Lactones

The antineoplastic sesquiterpene lactones tehranolide (**69**) and artemisinin (**70**) (Chart 5), isolated from *Artemisia diffusa* Krasch. ex Poljak (Asteraceae) and other *Artemisia* species, revealed their important anti-CaM effects through the change on fluorescence emission spectra of the protein and CaM-mediated activation of PDE1.(56) It was found that **69** has a higher inhibition constant (K_d = 6.1 μM) than **70** (K_d = 10 μM). In addition, **69** significantly reduces cell proliferation in a time- and dose-dependent manner in K562 cells, without affecting the growth of peripheral lymphocytes, as indicated in a cytotoxic assay.(56)

Natural Antimitotic Drugs

The interaction of Ca^{2+}-CaM with the alkaloidal antimitotic drugs vinblastine and vincristine has been demonstrated by using different spectroscopic techniques, including circular dichroism and fluorescence-based methods.(38) However, the direct effect on Ca^{2+}-*h*CaM of other antimitotic drugs such as paclitaxel (Taxol), griseofulvin, and colchicine has not been demonstrated yet. When vinblastine, vincristine, and colchicine were tested with the Ca^{2+}-Ca2+-*h*CaM M124C-*mBBr* biosensor, they quenched, in a concentration-dependent manner, the fluorescence of the device (K_d = 1.7, 0.80, and 0.50 μM, respectively). On the other hand, paclitaxel and griseofulvin, which share the same antimitotic mechanism, including increase of microtubule polymerization, did not induce quenching of Ca^{2+}-*h*CaM M124C-*mBBr*.(57, 58) The implications of these results remain to be determined.

Concluding Remarks

The recent literature concerning anti-CaM natural products has been updated in this review. In most cases, the activity observed correlated well with the known pharmacological properties of the compounds. A few inhibitors in the nanomolar potency range were detected using recently designed fluorescent biosensors. These tools are important technological developments and represent the state of the art for detecting new and potent CaM inhibitors in a very sensitive and specific fashion. The most active compounds were isolated from the fungal kingdom, which thus represent a valuable source of new and potent CaM antagonists in comparison to plant constituents. Therefore, these compounds represent leads for the development of new drugs as well as valuable research tools for understanding anti-CaM mechanisms.

Notes

[#] Adapted from a Norman R. Farnsworth Research Achievement Award address, 55th Annual Meeting of the American Society of Pharmacognosy, Oxford, Mississippi, August 2–6, 2014.

The authors declare no competing financial interest.

Dedicated to Dr. William Fenical of Scripps Institution of Oceanography, University of California–San Diego, for his pioneering work on bioactive natural products.

References

1. Chin, D.; Means, A. R. Trends Cell Biol. **2000**, 10, 322– 328
2. Berchtold, M. W.; Villalobo, A. Biochim. Biophys. Acta **2014**, 1843, 398– 435
3. Martinez-Luis, S.; Perez-Vásquez, A.; Mata, R. Phytochemistry **2007**, 68, 1882– 1903
4. Mata, R.; Figueroa, M.; Rivero-Cruz, I.; González-Andrade, M. In Bioactive Compounds from Natural Sources; Tringali, C., Ed.; CRC Press: Boca Raton, FL, **2012**; Chapter 13, pp 451– 496.
5. Sharma, R. K.; Wang, J. H. Adv. Cyclic Nucl. Res. **1979**, 10, 187– 198
6. Leung, P. C.; Taylor, W. A.; Wang, J. H.; Tipton, C. L. J. Biol. Chem. **1984**, 259, 2742– 2747

7. Ovadi, J. Prog. Drug Res. **1989**, 33, 353– 395

8. Molnar, A.; Liliom, K.; Orosz, F.; Vertessy, B. G.; Ovadi, J. Eur. J. Pharmacol. **1995**, 291, 73– 82

9. Au, T. K.; Leung, P. C. Plant Physiol. **1998**, 118, 965– 973

10. Vertessy, B. G.; Harmat, V.; Bocskei, Z.; Naray-Szabo, G.; Orosz, F.; Ovadi, J. Biochemistry **1998**, 37, 15300– 15310

11. Horvath, I.; Harmat, V.; Perczel, A.; Palfi, V.; Nyitray, L.; Nagy, A.; Hlavanda, E.; Naray-Szabo, G.; Ovadi, J. J. Biol. Chem. **2005**, 280, 8266– 8274

12. Ishima, R.; Torchia, D. A. Nat. Struct. Biol. **2000**, 7, 740– 743

13. Pelton, J. T.; McLean, L. R. Anal. Biochem. **2000**, 277, 167– 176

14. Uzawa, T.; Akiyama, S.; Kimura, T.; Takahashi, S.; Ishimori, K.; Morishima, I.; Fujisawa, T. Proc. Natl. Acad. Sci. U.S.A. **2004**, 101, 1171– 1176

15. Lipfert, J.; Doniach, S. Annu. Rev. Biophys. Biomed. **2007**, 36, 307– 327

16. Gilli, R.; Lafitte, D.; Lopez, C.; Kilhoffer, M.; Makarov, A.; Briand, C.; Haiech, J. Biochemistry **1998**, 37, 5450– 5456

17. Brokx, R. D.; Lopez, M. M.; Vogel, H. J.; Makhatadze, G. I. J. Biol. Chem. **2001**, 276, 14083– 14091

18. Hall, W. P.; Modica, J.; Anker, J.; Lin, Y.; Mrksich, M.; Van Duyne, R. P. Nano Lett. **2011**, 11, 1098– 1105

19. Coan, K. E.; Swann, M. J.; Ottl, J. Anal. Chem. **2012**, 84, 1586– 1591

20. Ma, L.; Wang, Z.; Liu, S.; Song, F.; Liu, Z. Rapid Commun. Mass Spectrom. **2013**, 27, 1527– 1534

21. Truong, K.; Ikura, M. Curr. Opin. Struct. Biol. **2001**, 11, 573– 578

22. Heyduk, T. Curr. Opin. Biotechnol. **2002**, 13, 292– 296

23. Axelrod, D. Traffic **2001**, 2, 764– 774

24. González-Andrade, M.; Figueroa, M.; Rodríguez-Sotres, R.; Mata, R.; Sosa-Peinado, A. Anal. Biochem. **2009**, 387, 64– 70

25. González-Andrade, M.; Rivera-Chávez, J.; Sosa-Peinado, A.; Figueroa, M.; Rodráguez-Sotres, R.; Mata, R. J. Med. Chem. **2011**, 54, 3875– 3884

26. Madariaga-Mazón, A.; González-Andrade, M.; Toriello, C.; Navarro-Barranco, H.; Mata, R.Nat. Prod Commun. **2014**, in press

27. Leyte-Lugo, M.; Figueroa, M.; González, M. C.; Glenn, A. E.; González-Andrade, M.; Mata, R. Phytochemistry **2013**, 96, 273– 278

28. Madariaga-Mazón, A.; González-Andrade, M.; González, M. D.; Glenn, A. E.; Cerda-Garcia-Rojas, C. M.; Mata, R. J. Nat. Prod. **2013**, 76, 1454– 1460

29. Estrada, S.; Rojas, A.; Mathison, Y.; Israel, A.; Mata, R. Planta Med. **1999**, 65, 109– 114

30. Estrada, S.; Toscano, R. A.; Mata, R. J. Nat. Prod. **1999**, 62, 1175– 1178

31. Hernández, Y.; Rojas, J. I.; Castillo, R.; Rojas, A.; Mata, R. J. Nat. Prod. **2004**, 67, 160– 167

32. Estrada, S.; Lopéz-Guerrero, J. J.; Villalobos-Molina, R.; Mata, R. Fitoterapia **2004**, 75, 690– 695

33. Rendón-Vallejo, P.; Hernández-Abreu, O.; Vergara-Galicia, J.; Ibarra-Barajas, M.; Estrada-Soto, S. J. Nat. Prod. **2012**, 75, 2241– 2245

34. Webb, R. C. Adv. Physiol. Educ. **2003**, 27, 201– 206

35. Reyes-Ramírez, A.; Leyte, M.; Figueroa, M.; Serrano, T.; González-Andrade, M.; Mata, R. Eur. J. Med. Chem. **2011**, 46, 2699– 2708

36. Morris, G. M.; Goodsell, D. S.; Halliday, R. S.; Huey, R.; Hart, W. E.; Belew, R. K.; Olson, A. J. J. Comput. Chem. **1998**, 19, 1639– 1662

37. Huey, R.; Morris, G. M.; Olson, A. J.; Goodsell, D. S. J. Comput. Chem. **2007**, 28, 1145– 1152

38. Harmat, V.; Böcskei, Z.; Náray-Szabó, G.; Bata, I.; Csutor, A. S.; Hermecz, I.; Arányi, P.; Szabó, B.; Liliom, K.; Vértessy, B. G.; Ovádi, J. J. Mol. Biol. **2000**, 297, 747– 755

39. Martínez-Luis, S.; Rodríguez, R.; Acevedo, L.; González, M. C.; Lira-Rocha, A.; Mata, R. Tetrahedron **2006**, 62, 1817– 1822

40. Figueroa, M.; González, M. C.; Mata, R. Nat. Prod. Res. **2008**, 22, 709– 714

41. Figueroa, M.; González-Andrade, M.; Sosa-Peinado, A.; Madariaga-Mazón, A.; Del Río-Portilla, F.; González, M. C.; Mata, R. J. Enzym. Inhib. Med. Chem. **2011**, 26, 378– 385

42. Madariaga-Mazón, A.; Hernández-Abreu, O.; Estrada-Soto, S.; Mata, R.J. Pharm. Pharmacol. **2014**, in press

43. González-Andrade, M.; Mata, R.; Madariaga-Mazán, A.; Rodríguez-Sotres, R.; Del Pozo-Yauner, L.; Sosa-Peinado, A. J. Mol. Recognit. **2013**, 26, 165– 174

44. Figueroa, M.; Del Carmen González, M.; Rodríguez-Sotres, R.; Sosa-Peinado, A.; González-Andrade, M.; Cerda-García-Rojas, C. M.; Mata, R. Bioorg. Med. Chem. **2009**, 17, 2167– 2174

45. Horvath, I.; Harmat, V.; Perczel, A.; Palfi, V.; Nyitray, L.; Nagy, A.; Hlavanda, E.; Naray-Szabo, G.; Ovadi, J. J. Biol. Chem. **2005**, 280, 8266– 8274

46. Ayers, S.; Graf, T. N.; Adcock, A. F.; Kroll, D. J.; Shen, Q.; Swanson, S. M.; Matthew, S.; Carcache de Blanco, E. J.; Wani, M. C.; Darveaux, B. A.; Pearce, C. J.; Oberlies, N. H. J. Antibiot. **2012**, 65, 3– 8

47. Leyte-Lugo, M.; González-Andrade, M.; González, M. C.; Glenn, A. E.; Cerda-García-Rojas, C. M.; Mata, R. J. Nat. Prod. **2012**, 75, 1571– 1577

48. Lorke, D. Arch. Toxicol. **1983**, 54, 275– 287

49. González-Andrade, M.; Del Valle, P. Chem. Biodiversity **2013**, 10, 328– 337

50. Shrimali, D.; Shanmugam, M. K.; Kumar, A. P.; Zhang, J.; Tan, B. K. H.; Ahn, K. S.; Sethi, G. Cancer Lett. **2013**, 341, 139– 149

51. Macías, M.; Ulloa, M.; Gamboa, A.; Mata, R. J. Nat. Prod. **2000**, 63, 757– 761

52. Macías, M.; Gamboa, A.; Ulloa, M.; Toscano, R. A.; Mata, R. Phytochemistry **2001**, 58, 751– 758

53. Mata, R.; Gamboa, A.; Macías, M.; Santillán, S.; Ulloa, M.; González, M. C. J. Agric. Food Chem. **2003**, 51, 4559– 4562

54. Ma, C.; Tang, K.; Liu, Q.; Zhu, R.; Cao, Z. Chem. Biol. Drug Des. **2013**, 81, 775– 783

55. Torres-Piedra, M.; Figueroa, M.; Hernández-Abreu, O.; Ibarra-Barajas, M.; Navarrete-Vázquez, G.; Estrada-Soto, S. Bioorg. Med. Chem. **2011**, 19, 542– 546

56. Noori, S.; Hassan, Z. M. Tumor Biol. **2014**, 35, 257– 264

57. Panda, D.; Rathinasamy, H.; Santra, M. K.; Wilson, L. Proc. Natl. Acad. Sci. U.S.A. **2005**, 102, 9878– 9883

58. Lu, Y.; Chen, J.; Xiao, M.; Li, W.; Miller, D. D. Pharm. Res. **2012**, 29, 2943– 2971